



Multimodel assessment of water scarcity under climate change

Jacob Schewe^{a,1}, Jens Heinke^{a,b}, Dieter Gerten^a, Ingjerd Haddeland^c, Nigel W. Arnell^d, Douglas B. Clark^e, Rutger Dankers^f, Stephanie Eisner^g, Balázs M. Fekete^h, Felipe J. Colón-Gonzálezⁱ, Simon N. Gosling^j, Hyungjun Kim^k, Xingcai Liu^l, Yoshimitsu Masaki^m, Felix T. Portmann^{n,o}, Yusuke Satoh^p, Tobias Stacke^q, Qihong Tang^l, Yoshihide Wada^r, Dominik Wisser^s, Torsten Albrecht^a, Katja Frieler^a, Franziska Piontek^a, Lila Warszawski^a, and Pavel Kabat^{t,u}

^aPotsdam Institute for Climate Impact Research, 14412 Potsdam, Germany; ^bInternational Livestock Research Institute, Nairobi, Kenya; ^cNorwegian Water Resources and Energy Directorate, N-0301 Oslo, Norway; ^dWalker Institute for Climate System Research, University of Reading, Reading RG6 6AR, United Kingdom; ^eCentre for Ecology and Hydrology, Wallingford OX10 8BB, United Kingdom; ^fMet Office Hadley Centre, Exeter EX1 3PB, United Kingdom; ^gCenter for Environmental Systems Research, University of Kassel, 34109 Kassel, Germany; ^hCivil Engineering Department, The City College of New York, New York, NY 10031; ⁱAbdus Salam International Centre for Theoretical Physics, I-34151 Trieste, Italy; ^jSchool of Geography, University of Nottingham, Nottingham NG7 2RD, United Kingdom; ^kInstitute of Industrial Science, The University of Tokyo, 4-6-1 Komaba, Meguro, Tokyo 153-8505, Japan; ^lDepartment of Civil Engineering, The University of Tokyo, 7-3-1 Hongo, Bunkyo, Tokyo 113-8654, Japan; ^mInstitute of Geographic Sciences and Natural Resources Research, Chinese Academy of Sciences, Beijing 100101, China; ⁿCenter for Global Environmental Research, National Institute for Environmental Studies, Tsukuba 305-8506, Japan; ^oLOEWE Biodiversity and Climate Research Centre and Senckenberg Research Institute and Natural History Museum, 60325 Frankfurt am Main, Germany; ^pInstitute of Physical Geography, Goethe University Frankfurt, 60438 Frankfurt am Main, Germany; ^qMax Planck Institute for Meteorology, 20146 Hamburg, Germany; ^rDepartment of Physical Geography, Utrecht University, 3584 CS Utrecht, The Netherlands; ^sCenter for Development Research, University of Bonn, 53113 Bonn, Germany; ^tInternational Institute for Applied Systems Analysis, A-2361 Laxenburg, Austria; and ^uWageningen University and Research Centre, 6708, Wageningen, The Netherlands

Edited by Hans Joachim Schellnhuber, Potsdam Institute for Climate Impact Research, Potsdam, Germany, and approved August 13, 2013 (received for review January 31, 2013)

Water scarcity severely impairs food security and economic prosperity in many countries today. Expected future population changes will, in many countries as well as globally, increase the pressure on available water resources. On the supply side, renewable water resources will be affected by projected changes in precipitation patterns, temperature, and other climate variables. Here we use a large ensemble of global hydrological models (GHMs) forced by five global climate models and the latest greenhouse-gas concentration scenarios (Representative Concentration Pathways) to synthesize the current knowledge about climate change impacts on water resources. We show that climate change is likely to exacerbate regional and global water scarcity considerably. In particular, the ensemble average projects that a global warming of 2 °C above present (approximately 2.7 °C above preindustrial) will confront an additional approximate 15% of the global population with a severe decrease in water resources and will increase the number of people living under absolute water scarcity (<500 m³ per capita per year) by another 40% (according to some models, more than 100%) compared with the effect of population growth alone. For some indicators of moderate impacts, the steepest increase is seen between the present day and 2 °C, whereas indicators of very severe impacts increase unabated beyond 2 °C. At the same time, the study highlights large uncertainties associated with these estimates, with both global climate models and GHMs contributing to the spread. GHM uncertainty is particularly dominant in many regions affected by declining water resources, suggesting a high potential for improved water resource projections through hydrological model development.

climate impacts | hydrological modeling | Inter-Sectoral Impact Model Intercomparison Project

Freshwater is one of the most vital natural resources of the planet. The quantities that humans need for drinking and sanitation are relatively small, and the fact that these basic needs are not satisfied for many people today is primarily a matter of access to, and quality of, available water resources (1). Much larger quantities of water are required for many other purposes, most importantly irrigated agriculture, but also for industrial use, in particular for hydropower and the cooling of thermoelectric power plants (2, 3). These activities critically depend on a sufficient amount of freshwater that can be withdrawn from rivers, lakes, and groundwater aquifers. Whereas scarcity of freshwater

resources already constrains development and societal well-being in many countries (4, 5), the expected growth of global population over the coming decades, together with growing economic prosperity, will increase water demand and thus aggravate these problems (6–8).

Climate change poses an additional threat to water security because changes in precipitation and other climatic variables may lead to significant changes in water supply in many regions (6–11). The effect of climate change on water resources is, however, uncertain for a number of reasons. Climate model projections, although rather consistent in terms of global average changes, disagree on the magnitude, and in many cases even the sign, of change at a regional scale, in particular when it comes to precipitation patterns (12). In addition, the way in which precipitation changes translate into changes in hydrological variables such as surface or subsurface runoff and river discharge (i.e., runoff accumulated along the river network), and thus in renewable water resources, depends on many biophysical characteristics of the affected region (e.g., orography, vegetation, and soil properties) and is the subject of hydrological models, which represent a second level of uncertainty (11, 13).

In the framework of the Inter-Sectoral Impact Model Intercomparison Project [ISI-MIP; Warszawski et al. (14) in this issue of PNAS] a set of nine global hydrological models, one global land-surface model, and one dynamic global vegetation model [here summarized as global hydrological models (GHMs); *Materials and Methods*] has been applied using bias-corrected forcing from five different global climate models (GCMs) under the newly developed Representative Concentration Pathways (RCPs). The purpose is to explore the associated uncertainties and to synthesize the current state of knowledge about the impact of climate change on renewable water resources at the global scale. In this paper we investigate the multimodel

Author contributions: J.S., K.F., F.P., L.W., and P.K. designed research; J.S., J.H., D.G., I.H., N.A., D.B.C., R.D., S.E., B.M.F., F.J.C.-G., S.N.G., H.K., X.L., Y.M., F.T.P., Y.S., T.S., Q.T., Y.W., and D.W. performed research; J.S. and T.A. analyzed data; and J.S. wrote the paper.

The authors declare no conflict of interest.

This article is a PNAS Direct Submission.

¹To whom correspondence should be addressed. E-mail: jacob.schewe@pik-potsdam.de.

This article contains supporting information online at www.pnas.org/lookup/suppl/doi:10.1073/pnas.1222460110/-DCSupplemental.

ensemble projections and the associated spread for changes in annual discharge—taken here as a first-order measure of the water resources available to humans. We then reconcile these hydrological changes with global population patterns to estimate how many people will be living in areas affected by a given change in water resources. Finally, we apply a commonly used measure of water scarcity to estimate the percentage of the world's population living in water-scarce countries and to quantify the contributions of both climate change and population change to the change in water scarcity. Results are presented as a function of global mean warming above the present day to account for the relative independence of regional temperature, precipitation, and runoff changes of the rate of warming (15, 16) and to allow for systematic comparison of climate change impacts across scenarios and sectors.

Results

Discharge Trends and Uncertainties. We first consider the spatial pattern of relative change in annual mean discharge at 2 °C global warming compared with present day (the term “present day” in this study refers to the 1980–2010 average, which is ~0.7 °C warmer globally than preindustrial), under RCP8.5 (Fig. 1). The multimodel mean across all GHMs and GCMs (Fig. 1, *Upper*) exhibits a number of robust large-scale features. In particular, discharge is projected to increase at high northern latitudes, in eastern Africa and on the Indian peninsula, and to decrease in a number of regions including the Mediterranean and large parts of North and South America. In these regions,

a relatively high level of agreement across the multimodel ensemble on the sign of change indicates high confidence. Most of these patterns are consistent with previous studies (8, 11, 17, 18), but there are also some differences. For example, ensemble projections using the previous generation of GCMs and climate scenarios found a robust runoff increase in southeastern South America (19, 20), where we find no clear trend, or partly even a drying trend. Whereas those latter studies used larger GCM ensembles, we apply an unprecedented number of GHMs as well as the new RCP climate forcing. At 3 °C of global mean warming, the pattern of change is similar to that at 2 °C, although the changes are enhanced in many regions, and new robust trends emerge in some regions (most notably a strong negative trend in Mesoamerica; *SI Appendix, Fig. S1*).

In other parts of the globe, however, the projections are subject to a large spread across the ensemble. In many regions, forcing by different GCMs yields discharge changes (averaged across GHMs) that are large but of opposite sign (*SI Appendix, Fig. S2* shows individual maps of precipitation and discharge changes). Accordingly, the spread owing to differences between GCMs dominates the total ensemble spread in these regions (Fig. 1, *Lower*). By contrast, GHM spread is dominant in many regions that are subject to discharge reductions (e.g., northern and southern Africa). In most other regions showing a large total spread, GHMs and GCMs contribute about equally. Note that the bias correction applied to the GCM data (*Materials and Methods*) substantially reduces the spread among the GCMs' present-day climatologies, but not among their future temperature and precipitation trends (21).

Population Affected by Severe Changes in Water Resources. To put these discharge changes into a societal perspective, we reconcile them with the spatial distribution of population, using population projections from the newly developed Shared Socioeconomic Pathways (SSPs) (22). In the following, we will focus on the middle-of-the-road population scenario according to SSP2, which projects global population to increase up to a peak at around 10 billion by the year 2090 and includes substantial changes in relative population densities among countries; constant present-day population will be considered additionally as a reference case.

We first consider two criteria for a severe decrease in average annual discharge, as an indicator of renewable water resources: a reduction by more than 20% and a reduction by more than 1 SD (σ) of 1980–2010 annual discharge. Both criteria can be seen as first-order indicators of when available water resources consistently fall short of what a given population has adapted to and thus serious adaptation challenges are likely to arise. In many cases, a given discharge decrease may be detected using either criterion. In regions where interannual variability is high but baseline discharge is low, the first criterion is particularly important because even discharge reductions smaller than 1 σ can aggravate water stress significantly in these regions. Conversely, in regions with low interannual variability, the second criterion detects low-amplitude changes that may nonetheless require substantial adaptation action as they transgress the range of past variability [e.g., in central and western Africa; Piontek et al. (23) in this issue of PNAS]. Based on grid-cell discharge averaged over 31-y periods that correspond to a given level of global warming, and on gridded population projections (*Materials and Methods* and *SI Appendix, Table S1*), we compute the percentage of global population living in countries with a discharge reduction according to either or both of the criteria (Fig. 2). With global mean warming on the horizontal axis, the differences between the different RCPs in this population-weighted metric, as well as in globally averaged runoff, are small and in the range of interdecadal variability (*SI Appendix, Fig. S3*), meaning that these global, long-term indicators do not depend strongly on the rate of global warming. We therefore concentrate on RCP8.5.

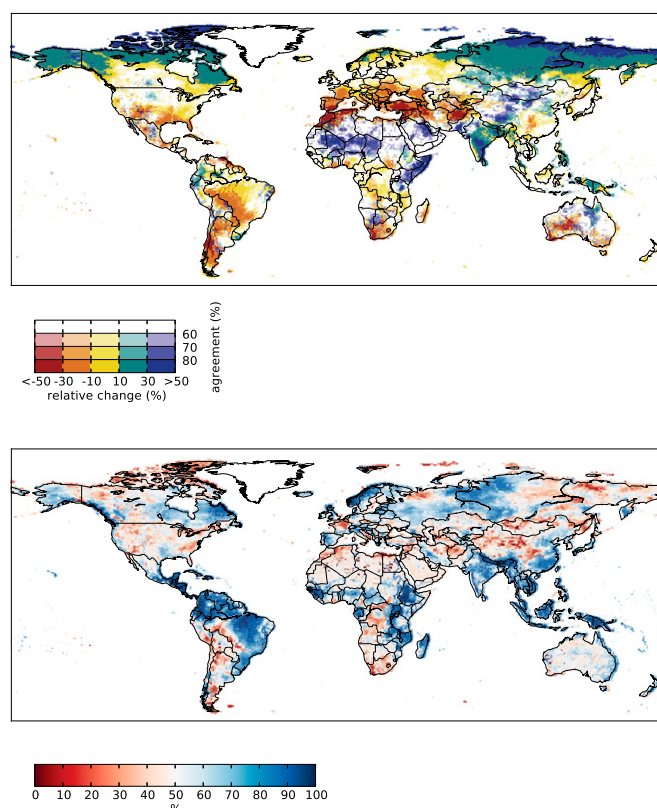


Fig. 1. Relative change in annual discharge at 2 °C compared with present day, under RCP8.5. (*Upper*) Color hues show the multimodel mean change, and saturation shows the agreement on the sign of change across all GHM–GCM combinations (percentage of model runs agreeing on the sign; color scheme following ref. 58). (*Lower*) Ratio of GCM variance to total variance; in red (blue) areas, GHM (GCM) variance predominates. GHM variance was computed across all GHMs for each GCM individually, and then averaged over all GCMs; vice versa for GCM variance. Greenland has been masked.

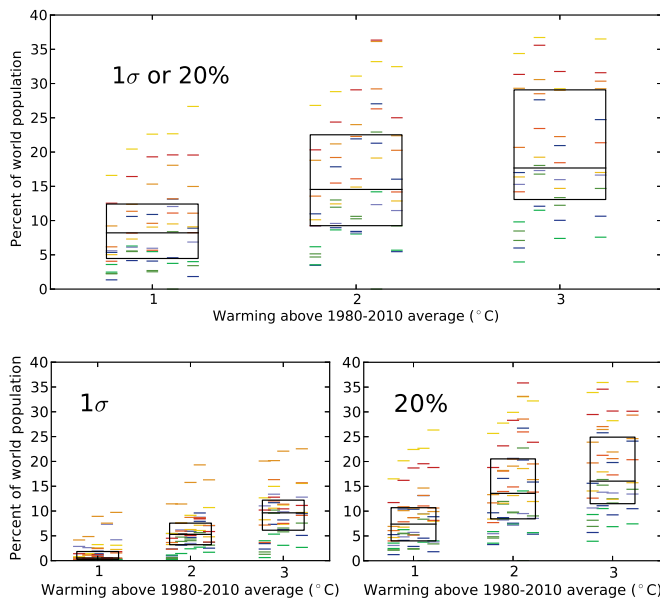


Fig. 2. Adverse impact of climate change on renewable water resources at different levels of global warming. Markers show the percentage of the world population living in $0.5^\circ \times 0.5^\circ$ grid cells where the 31-y average of annual discharge falls short of the 1980–2010 average by more than 1σ (SD of annual discharge during 1980–2010), or by more than 20%, under the RCP8.5 climate scenario and SSP2 population scenario. The five GCMs are displayed in separate vertical columns (in the order in which they are listed in *Materials and Methods*; note that only four GCMs have sufficient coverage of the 3 °C warming level), and the 11 GHMs are displayed in unique colors. The black boxes give the interquartile range, and the horizontal black lines the median, across all GCMs and GHMs.

(the only RCP compatible with >3 °C warming by 2100) to span a large range of temperature levels, while noting that on smaller spatial and temporal scales larger dependencies on the warming rate as well as on climate model internal variability might be observed (24).

The multimodel median (MMM) suggests that even a relatively modest global warming of 1 °C above present day will lead to a severe reduction in water resources, by at least one of the two criteria, for about 8% of the global population. This figure rises to about 14% for 2 °C and 17% for 3 °C. When only one criterion is applied, the numbers are somewhat smaller (Fig. 2, Lower): At 2 °C, about 13% (6%) of the global population is projected to experience a discharge reduction $>20\%$ ($>1\sigma$). When a stricter criterion of a discharge reduction $>40\%$ or $>2\sigma$ is used, about 5% of the global population is affected at 2 °C, according to the MMM (SI Appendix, Fig. S4).

Importantly, however, the spread across the multimodel ensemble is large. For a few GHM–GCM combinations, the figure for the 20% or 1σ criterion never exceeds 10%, whereas others project that more than 30% of the global population will already be affected at 2 °C. Note that in many of the regions that experience the strongest relative reduction in discharge, GHM variance is larger than GCM variance (Fig. 1, Lower). Accordingly, the spread across GHMs in Fig. 2 is comparable to or even larger than the spread across GCMs. Moreover, the two models included in the study that simulate vegetation distribution and dynamics (green markers in Fig. 2) yield generally smaller reductions in water resources than most stand-alone hydrological models, suggesting systematic differences between the two types of models (25). Sensitivity experiments confirm that the effect of additional CO₂ fertilization of vegetation on the hydrology is comparatively small (26) (SI Appendix, Fig. S5). Dynamic vegetation changes or details of the parameterizations of evapotranspiration may

contribute to the divergence as well, but this requires a more systematic investigation.

The metric discussed here (percentage of population experiencing a given discharge change) depends on the population scenario only through the geographical distribution of population, not through the global totals. Holding the total and the geographical distribution of population constant at the year-2000 level suggests slightly lower impacts, indicating that under SSP2 the population increase is, on average, somewhat stronger in regions affected by discharge reductions than in other regions (SI Appendix, Fig. S4). This, however, has only a relatively small effect at the global scale.

As seen in the previous section, the projected changes in discharge are regionally very heterogeneous, with water resources decreasing in many regions but increasing in others. Grouping the world population into categories of percentage discharge change (e.g., 10–30% increase/decrease, measured by the multimodel mean; SI Appendix, Fig. S6), the number of people falling into a given increase category is often very similar to the number of people falling into the corresponding decrease category. Combined with up to ~15% of the global population who are projected to experience increases exceeding 100% of today's discharge, overall more people will be affected by discharge increases than will be by decreases. Whereas such increases may enhance actual water availability in many cases, they can also entail adverse impacts such as increasing flood risk, deteriorating water quality, and malfunctioning of water-related infrastructure (27).

Water Scarcity. The impact metric considered in the previous section measures, at the grid-cell level, significant departures from present levels of resource availability, irrespective of what those levels are. It is thus an indicator of adaptation challenges that may arise, but not necessarily of resource scarcity in an absolute sense. Moreover, because most water is used for irrigated agriculture, which does not necessarily take place in the same location where people live, water scarcity can be assessed more appropriately on a larger spatial scale than on the grid-cell level. A widely used, simple indicator of water scarcity, the water crowding index (28, 29), relates water resources to population at the country scale. Defined originally as the number of people depending on a given resource unit, we use the inverse (i.e., annual mean water resources per capita). Considering only supply-side changes, this indicator is suitable for assessing the impact of climate change on physical water scarcity, whereas the actual water stress experienced by people will also depend on changes in per-capita water requirements and uses (30). We base our water scarcity assessment on the “blue” water (BW) resource (31), defined here as runoff redistributed across the river basin according to the distribution of discharge (*Materials and Methods*). Compared with using discharge itself, this avoids counting a given water unit more than once, while retaining the spatial distribution of discharge across the basin. The latter is important, for example, in countries like Egypt, where most of the available water resource is generated by runoff outside the country (in this case, in the Nile River headwaters).

We consider the percentage of global population in either of two water scarcity classes: annual BW availability below 500 m³ per capita (also termed absolute water scarcity) and below 1,000 m³ per capita (chronic water scarcity). The MMM suggests that at present ~1.5% and ~3% of the global population fall into these two scarcity classes, respectively (the first class being a subset of the second; Fig. 3A and B). This is similar to previous estimates at the country level (7) but much lower than estimates done at the grid-cell level (4, 17) or river basin level (7) because larger countries may not be classified as water-scarce even though significant parts of their population live in water-scarce grid cells. Whereas the country level might in some cases be too coarse for a realistic assessment of water scarcity and generally

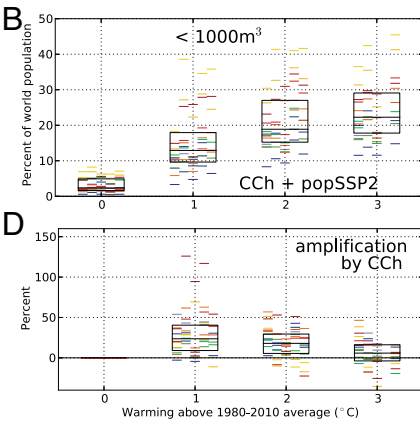
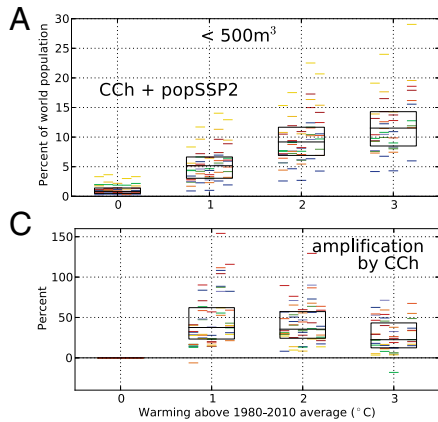


Fig. 3. Percentage of world population living in countries with annual mean BW availability (*Materials and Methods*) below 500 m^3 per capita (Left) and below $1,000 \text{ m}^3$ per capita (Right). Symbols as in Fig. 2. (A and B) RCP8.5 climate scenario, population change according to SSP2. (C and D) Amplification by climate change of the level of water scarcity that is expected from population change alone; computed as the difference between a constant-climate scenario (*SI Appendix, Fig. S7*) and the full scenario shown above, divided by the constant-climate scenario, and expressed as percentage (so that the population-only case equals 100%). For example, in C, the MMM indicates that at 2°C global warming, climate change amplifies the level of absolute water scarcity (number of people below 500 m^3 per capita) expected from population change alone by about 36%.

underestimate the global figure, the grid-cell level likely overestimates it because water transfers between grid cells [and also virtual water imports related to trade of water-intensive goods (32)] are large in reality.

Our present-day estimate is already subject to a significant spread across the multimodel ensemble (ranging from 0 to 4% for the $<500 \text{ m}^3$ class and 1–8% for the $<1,000 \text{ m}^3$ class), owing mainly to differences in present-day discharge simulated by the different GHMs (13). The present-day discharge estimates also depend to a certain extent on the observation-based dataset that was used for bias-correcting the climate input data (*Materials and Methods*). Under the SSP2 population scenario (and again using 31-y averages associated with the different warming levels), the percentage of people living in countries below 500 m^3 per capita ($1,000 \text{ m}^3$ per capita) is projected to rise to 6% (13%) at 1°C , 9% (21%) at 2°C , and 12% (24%) at 3°C of global warming, according to the MMM (Fig. 3A and B). The high rates of rise between present-day and 1°C could be partly related to the fact that the present-day estimate is very low, and different spatial scales of analysis may lead to different relative changes.

Population growth plays a major role in this increase in water scarcity because it reduces per-capita availability even with unchanged resources. To separate the population signal from the climate signal, we use each model combination's average 1980–2010 discharge pattern to compute the percentage of people that would fall into a scarcity class if climate were to remain constant and population changed according to SSP2 (*SI Appendix, Fig. S7*).

As found in previous studies (6, 31, 33), population change explains the larger part of the overall change in water scarcity. Subtracting the constant-climate scenario from the full scenario and dividing by the constant-climate scenario indicates by how much the level of water scarcity expected owing to population change alone is amplified by climate change (Fig. 3 C and D). According to the MMM, this amplification is nearly 40% for the $<500 \text{ m}^3$ class at 1°C and 2°C global warming. The factor is somewhat lower (approximately 25%) at 3°C , indicating that at this level of warming the effect of additional climate change on this global metric becomes smaller compared with the effect of population changes. Note that this is partly related to the relative timing of warming and population change: In an even faster-warming scenario than RCP8.5, a warming from 2°C to 3°C might still have a relatively larger impact because it would be associated with generally lower population numbers. This observation illustrates how climate change and population change combine to aggravate global water scarcity: A country can move toward the water scarcity threshold both through population growth and through declining water resources, and depending on the relative rates of change, it may be one or the other factor that eventually causes the threshold to be crossed.

Along similar lines, for the $\leq 1,000 \text{ m}^3$ class, the MMM amplification due to climate change is nearly 30% at 1°C , drops to about 20% at 2°C , and is close to zero at 3°C . A number of model combinations yield negative values in Fig. 3 C and D; in these cases, climate change is projected to alleviate the global increase in water-scarce population that is expected owing to population change. The GHMs projecting a positive effect of climate change on chronic water scarcity (i.e., yielding negative values in Fig. 3D) are primarily models that show a large number of people in this scarcity class in the first place (yellow and red markers in Fig. 3B). This suggests that in these models many countries in regions that get drier are already in this class at present, such that the potential for additional countries to move into the class is smaller compared with the potential for countries to move out of the class in regions that get wetter.

Discussion

Our multimodel assessment adds to extensive previous work, in particular in the framework of the European Union Integrated Project Water and Global Change (EU-WATCH) and Water Model Intercomparison Project (WaterMIP) (13), which demonstrated that hydrological models are a significant source of uncertainty in projections of runoff and evapotranspiration (11). The present study, using a larger ensemble ensemble of GHMs and GCMs and the state-of-the-art RCP climate forcing available from Coupled Model Intercomparison Project Phase 5 (CMIP-5), explores the range of uncertainty not only in hydrological change but also in its effect on people. Results are mapped against global mean temperature increase to allow direct comparison of the impacts at different levels of global warming.

It is important to note that our globally aggregated water scarcity estimates can obscure potentially much more severe changes at the scale of individual countries or locations. For example, if a number of countries were to move into a given water scarcity class, but at the same time other countries with a similar share of global population were to move out of this class, the resulting change on the global scale would be close to zero. Likewise, if the amplification of the global water scarcity signal by climate change becomes small at higher levels of warming, as seen in Fig. 3 C and D, this could mean that climate change continues to force additional countries into the scarcity class, but at the same time other countries move out of the class (e.g., because of more pronounced regional precipitation increases at this temperature level). The results in Fig. 3 must thus be interpreted with care, and the numbers in Fig. 3 C and D in particular are more likely to represent a lower bound to the climate change contribution in regions that are affected by a discharge decrease. Moreover, changes within a given water scarcity class are not detected here but can be very important. Countries

that are already extremely water-scarce will be all the more vulnerable to even small decreases in resource availability.

Although the water crowding index is an appropriate measure for supply-side effects on global water scarcity, it is not a measure of the actual problems that countries and people face in satisfying their water needs because it does not take the demand side into account. Future water stress (as measured, for instance, by the ratio of water use to availability) will depend on changes in demand, for example, related to economic growth, lifestyle changes, or technological developments, as well as on water management practices and infrastructure. Alternative sources of water for agriculture, such as “green” water contained in the soil (31, 33, 34), and nonrenewable water resources (35, 36), also affect actual BW requirements.

We have only considered long-term averages, neglecting potential changes in the interannual and seasonal availability of water resources and their variability (10, 37). Changes in seasonality can have severe impacts even if the annual average is stable e.g., if irrigation water availability in the growing season changes, or if flood hazard is affected by changes in snow-melt runoff [Dankers et al. (38) in this issue of PNAS]. Again, infrastructure such as dams and reservoirs can substantially alter the timing of water resource availability (39). Moreover, hydrological changes can have consequences going far beyond the availability of water resources for human uses, for instance, by altering the occurrence of damaging extreme events like floods and droughts [Prudhomme et al. (40) in this issue of PNAS], affecting aquatic and terrestrial ecosystems (41), and potentially interacting with, and amplifying, climate change impacts in other sectors (42).

Conclusions

We have synthesized results from 11 GHMs with forcing from five GCMs to provide an overview of the state of the art of modeling the impact of climate change on global water resources. In all metrics considered, we find a considerable spread across the simulation ensemble. GHMs and GCMs contribute to similar extents to the spread in relative discharge changes globally. When changes in water scarcity are considered, GHM spread is in fact larger than GCM spread. This finding suggests that, although climate model uncertainty remains an important concern, further impact model development promises major improvements in water scarcity projections.

The multimodel mean projected changes in annual discharge are spatially heterogeneous. As the planet gets warmer, a rising share of the world population will be affected by severe reductions in water resources, measured as deviation from present-day discharge in terms of either SD or percentage. However, a similar fraction of the population will experience increases in average discharge, which could potentially improve water availability, but also entail adverse effects.

Our estimate of water scarcity at the country scale indicates that climate change may substantially aggravate the water scarcity problem. Depending on the rates of both population change and global warming, the level of water scarcity expected owing to population change alone is amplified by up to 40% owing to climate change, according to the multimodel mean; some models suggest an amplification by more than 100%. This adds up to between 5% and 20% of global population likely exposed to absolute water scarcity at 2 °C of global warming. For chronic water scarcity, most adverse climate change impacts already occur between present day and 2 °C, whereas beyond this temperature positive and negative additional impacts of climate change are of a similar magnitude (although they affect different groups of people and therefore cannot be offset against each other). However, absolute water scarcity continues to be substantially amplified by climate change on the global scale even beyond 2 °C. We conclude that the combination of unmitigated

climate change and further population growth will expose a significant fraction of the world population to chronic or absolute water scarcity. This dwindling per-capita water availability is likely to pose major challenges for societies to adapt their water use and management.

Materials and Methods

Models and Data. The GHMs used in this study are the DBH (43), H08 (44), Mac-PDM.09 (45), MATSIRO (46), MPI-HM (47), PCR-GLOBWB (36), VIC (48), WaterGAP (49), and WBMplus (50) hydrological models, the JULES (51) land-surface model, and the LPJmL (52) dynamic global vegetation model; the latter two also represent vegetation dynamics in addition to hydrological processes. *SI Appendix, Table S2* gives further model details. Forcing data were derived from climate projections with the HadGEM2-ES, IPSL-CM5A-LR, MIROC-ESM-CHEM, GFDL-ESM2M, and NorESM1-M GCMs under the RCPs (53), which were prepared for the CMIP-5 (54). All required climate variables have been bias-corrected (55) toward an observation-based dataset (56) using a newly developed method (21) that builds on earlier approaches (57) but was specifically designed to preserve the long-term trends in temperature and precipitation projections to facilitate climate change studies. GHMs were run without direct coupling to GCMs, so that potential feedbacks (e.g., from GHM-simulated evapotranspiration on precipitation) were not represented. Further details about the GHM simulations can be found in the ISI-MIP simulation protocol available at <http://www.isi-mip.org/>. Country-level United Nations World Population Prospects (historical) and SSP (projections) population data at a 5-y time step were obtained from the SSP Database at <https://secure.iiasa.ac.at/web-apps/ene/SspDb> and linearly interpolated to obtain annual values. A gridded population dataset was also used in which the National Aeronautics and Space Administration GPWv3 y-2010 gridded population dataset (<http://sedac.ciesin.columbia.edu/data/collection/gpw-v3>) was scaled up to match the SSP country totals (neglecting changes in population distribution within countries).

Temperature Axis. Global mean temperature is calculated from the GCM data (including ocean cells) and presented as the difference from the 1980–2010 average. For each GCM and RCP, 31-y periods are selected whose average temperature corresponds to the different levels of global warming (*SI Appendix, Table S1*; note that GFDL-ESM2M does not reach the 3 °C warming level). Population affected by discharge changes (Fig. 2) was calculated using the population distribution corresponding to the middle year of each individual 31-y period (except for the baseline period 1980–2010, which was assumed to correspond to year-2000 population). Water scarcity (Fig. 3) was calculated annually, using annual population values, and then averaged over the 31-y periods; results for the 0 °C baseline were obtained from the “constant-climate” run, that is, using 1980–2010 average BW resources and annual population values (discussed in the following section).

Water Scarcity. For assessing country-scale water scarcity, we calculate the annual mean BW resource availability following ref. 31: The sum of annual mean runoff R in each river basin b is redistributed across the basin according to the relative distribution of discharge Q , yielding the BW resource in each grid cell i :

$$BW_i = R_b Q_i / \sum Q_i$$

where Σ is the sum over all grid cells in basin b . BW is then summed up over all grid cells within a country and divided by the country's population to yield the water crowding index. Finally, for each year, the total number of people living in countries that are below a given threshold of this index (500 m³ or 1,000 m³ per capita) is calculated and divided by global population to yield the corresponding percentage of world population. Results are again averaged over the 31-y periods that correspond to the different levels of global warming shown in Fig. 3 A and B. For the climate change contribution shown in Fig. 3 C and D, the subtraction of, and division by, the results from the constant-climate run is done year by year, and the resulting percentage is averaged over the 31-y periods.

Ensemble Statistics. Statistics across the multimodel ensemble were computed after the calculation of the respective metric. For instance, in Fig. 1 the relative change in discharge was calculated for each model combination individually before computing the multimodel mean, agreement, and variances.

ACKNOWLEDGMENTS. The authors acknowledge the World Climate Research Programme's Working Group on Coupled Modelling, which is responsible for

the Coupled Model Intercomparison Project, and thank the climate modeling groups for producing and making available their model output. J.S. wishes to thank A. Levermann for helpful discussions. This work has been conducted under the framework of the Inter-Sectoral Impact Model Intercomparison Project (ISI-MIP). The ISI-MIP Fast Track project underlying this paper was funded by the German Federal Ministry of Education and Research with project funding reference number 01LS1201A. R.D. was supported by the joint Department of Energy and Climate Change/Defra Met Office Hadley Centre Climate Programme (GA01101). F.J.C.-G. was jointly funded by the European Union Seventh Framework Programme Quantifying Weather and Climate Impacts on health in

developing countries and HEALTHY FUTURES projects. S.N.G. was supported by a Science, Technology and Society Priority Group grant from University of Nottingham. Y.M. was supported by the Environment Research and Technology Development Fund (S-10) of the Ministry of the Environment, Japan. F.T.P. received funding from the European Union's Seventh Framework Programme (FP7/2007-2013) under Grant 266992. K.F. was supported by the Federal Ministry for the Environment, Nature Conservation and Nuclear Safety, Germany (11_II_093_Global_A_SIDS and LDCs). H.K. and Y.S. were jointly supported by Japan Society for the Promotion of Science KAKENHI (23226012) and Ministry of Education, Culture, Sports, Science and Technology SOUSEI Program.

1. Ohlsson L, Turton AR (1999) The turning of a screw: Social resource scarcity as a bottleneck in adaptation to water scarcity. Occasional Paper Series, School of Oriental and African Studies Water Study Group, University of London.
2. Wallace J (2000) Increasing agricultural water use efficiency to meet future food production. *Agric Ecosyst Environ* 82(1-3):105–119.
3. Kummu M, Ward PJ, de Moel H, Varis O (2010) Is physical water scarcity a new phenomenon? Global assessment of water shortage over the last two millennia. *Environ Res Lett* 5(3):034006.
4. Oki T, et al. (2001) Global assessment of current water resources using total runoff integrating pathways. *Hydrol Sci J* 46(6):983–995.
5. Rijsberman F (2006) Water scarcity: Fact or fiction? *Agric Water Manage* 80:5–22.
6. Vörösmarty CJ, Green P, Salisbury J, Lammers RB (2000) Global water resources: Vulnerability from climate change and population growth. *Science* 289(5477):284–288.
7. Arnell NW (2004) Climate change and global water resources: SRES emissions and socio-economic scenarios. *Glob Environ Change* 14(3-4):31–52.
8. Alcamo J, Flörke M, Märker M (2007) Future long-term changes in global water resources driven by socio-economic and climatic changes. *Hydrol Sci J* 52(3):247–275.
9. Milly PCD, Dunne KA, Vecchia AV (2005) Global pattern of trends in streamflow and water availability in a changing climate. *Nature* 438(7066):347–350.
10. Fung F, Lopez A, New M (2011) Water availability in +2C and +4C worlds. *Philos Trans Ser A* 369(1934):99–116.
11. Hagemann S, et al. (2012) Climate change impact on available water resources obtained using multiple global climate and hydrology models. *Earth Syst Dynam Discuss* 3(3-4):1321–1345.
12. Meehl G, Stocker T, Collins W (2007) *Global Climate Projections* (Cambridge Univ Press, Cambridge, UK).
13. Haddeland I, et al. (2011) Multimodel estimate of the global terrestrial water balance: Setup and first results. *J Hydrometeorol* 12(5):869–884.
14. Warszawski L, et al. (2014) The Inter-Sectoral Impact Model Intercomparison Project (ISI-MIP): Project framework. *Proc Natl Acad Sci USA* 111:3228–3232.
15. Frieler K, Meinshausen M, Mengel M, Braun N, Hare W (2012) A scaling approach to probabilistic assessment of regional climate change. *J Clim* 25(4):3117–3144.
16. Tang Q, Lettenmaier DP (2012) 21st century runoff sensitivities of major global river basins. *Geophys Res Lett* 39(3):L06403.
17. Arnell NW, van Vuuren DP, Isaac M (2011) The implications of climate policy for the impacts of climate change on global water resources. *Glob Environ Change* 21(2):592–603.
18. Gosling SN, Bretherton D, Haines K, Arnell NW (2010) Global hydrology modelling and uncertainty: Running multiple ensembles with a campus grid. *Philos Trans Ser A* 368(1926):4005–4021.
19. Bates B, Kundzewicz Z, Wu S, Palutikof J (2008) Climate change and water. Technical paper of the Intergovernmental Panel on Climate Change (IPCC Secretariat, Geneva).
20. Füssel H, Heinke J, Popp A, Gerten D (2012) Climate change and water supply. *Climate Change, Justice and Sustainability: Linking Climate and Development Policy* (Springer, Dordrecht, The Netherlands), pp 19–32.
21. Hempel S, Frieler K, Warszawski L, Schewe J, Piontek F (2013) A trend-preserving bias correction the ISI-MIP approach. *Earth System Dynamics* 4(1):219–236.
22. Neill BCO, et al. (2012) Meeting report of the Workshop on the Nature and Use of New Socioeconomic Pathways for Climate Change Research, Boulder, CO, November 2–4, 2011.
23. Piontek F, et al. (2014) Multisectoral climate impact hotspots in a warming world. *Proc Natl Acad Sci USA* 111:3233–3238.
24. Heinke J, et al. (2012) A new dataset for systematic assessments of climate change impacts as a function of global warming. *Geoscientific Model Development Discussions* 5(4):3533–3572.
25. Davie JCS, et al. (2013) Comparing projections of future changes in runoff and water resources from hydrological and ecosystem models in ISI-MIP. *Earth System Dynamics Discussions* 4(1):279–315.
26. Piao S, et al. (2007) Changes in climate and land use have a larger direct impact than rising CO₂ on global river runoff trends. *Proc Natl Acad Sci USA* 104(39):15242–15247.
27. Kundzewicz ZW, et al. (2008) The implications of projected climate change for freshwater resources and their management. *Hydrol Sci J* 53(1):3–10.
28. Falkenmark M, Lundqvist J, Widstrand C (1989) Macro-scale water scarcity requires micro-scale approaches. Aspects of vulnerability in semi-arid development. *Nat Resour Forum* 13(4):258–267.
29. Falkenmark M, et al. (2007) *On the Verge of a New Water Scarcity* (Stockholm International Water Institute, Stockholm).
30. Ashton PJ (2002) Avoiding conflicts over Africa's water resources. *Ambio* 31(3):236–242.
31. Gerten D, et al. (2011) Global water availability and requirements for future food production. *J Hydrometeorol* 12(5):885–899.
32. Hanasaki N, Inuzuka T, Kanae S, Oki T (2010) An estimation of global virtual water flow and sources of water withdrawal for major crops and livestock products using a global hydrological model. *J Hydrol (Amst)* 384(3-4):232–244.
33. Rockström J, et al. (2009) Future water availability for global food production: The potential of green water for increasing resilience to global change. *Water Resour Res* 45:1–16.
34. Rost S, et al. (2008) Agricultural green and blue water consumption and its influence on the global water system. *Water Resour Res* 44(9):1–17.
35. Taylor RG, et al. (2012) Ground water and climate change. *Nature Climate Change* 3:322–329.
36. Wada Y, et al. (2010) Global depletion of groundwater resources. *Geophys Res Lett* 37(7):L20402.
37. Gosling SN, Taylor RG, Arnell NW, Todd MC (2011) A comparative analysis of projected impacts of climate change on river runoff from global and catchment-scale hydrological models. *Hydrol Earth Syst Sci* 15(7):279–294.
38. Dankers et al. (2014) First look at changes in flood hazard in the Inter-Sectoral Impact Model Intercomparison Project ensemble. *Proc Natl Acad Sci USA* 111:3257–3261.
39. Biemans H, et al. (2011) Impact of reservoirs on river discharge and irrigation water supply during the 20th century. *Water Resour Res* 47(3):1–15.
40. Prudhomme et al. (2014) Hydrological droughts in the 21st century: Hotspots and uncertainties from a global multimodel ensemble experiment. *Proc Natl Acad Sci USA* 111:3262–3267.
41. Gerten D, Schaphoff S, Lucht W (2007) Potential future changes in water limitations of the terrestrial biosphere. *Clim Change* 80(3-4):277–299.
42. Parry M, et al. (2001) Millions at risk: Defining critical climate change threats and targets. *Glob Environ Change* 11:181–183.
43. Tang Q, Oki T, Kanae S, Hu H (2007) The influence of precipitation variability and partial irrigation within grid cells on a hydrological simulation. *J Hydrometeorol* 8:499–512.
44. Hanasaki N, et al. (2008) An integrated model for the assessment of global water resources – Part 1: Model description and input meteorological forcing. *Hydrol Earth Syst Sci* 12(4):1007–1025.
45. Gosling SN, Arnell NW (2011) Simulating current global river runoff with a global hydrological model: Model revisions, validation, and sensitivity analysis. *Hydrol Processes* 25:1129–1145.
46. Takata K, Emori S, Watanabe T (2003) Development of the minimal advanced treatment of surface interaction and runoff. *Global Planet Change* 38(1-2):209–222.
47. Stacke T, Hagemann S (2012) Development and validation of a global dynamical wetlands extent scheme. *Hydrol Earth Syst Sci Discuss* 9(1):405–440.
48. Liang X, Lettenmaier DP, Wood EF, Burges SJ (1994) A simple hydrologically based model of land surface water and energy fluxes for general circulation models. *J Geophys Res* 99(D7):14415.
49. Döll P, Kaspar F, Lehner B (2003) A global hydrological model for deriving water availability indicators: model tuning and validation. *J Hydrol (Amst)* 270(1-2):105–134.
50. Wisser D, Fekete BM, Vörösmarty CJ, Schumann AH (2010) Reconstructing 20th century global hydrography: a contribution to the Global Terrestrial Network-Hydrology (GTN-H). *Hydrol Earth Syst Sci* 14(1):1–24.
51. Best MJ, et al. (2011) The Joint UK Land Environment Simulator (JULES), model description Part 1: Energy and water fluxes. *Geoscientific Model Development* 4(3):677–699.
52. Bondeau A, et al. (2007) Modelling the role of agriculture for the 20th century global terrestrial carbon balance. *Glob Change Biol* 13(3):679–706.
53. Moss RH, et al. (2010) The next generation of scenarios for climate change research and assessment. *Nature* 463(7282):747–756.
54. Taylor KE, Stouffer RJ, Meehl GA (2012) An overview of CMIP5 and the experiment design. *Bull Am Meteorol Soc* 93:485–498.
55. Ehret U, Zehe E, Wulfmeyer V, Warrach-Sagi K, Liebert J (2012) HESS opinions: Should we apply bias correction to global and regional climate model data? *Hydrol Earth Syst Sci* 16(9):3391–3404.
56. Weedon GP, et al. (2011) Creation of the WATCH forcing data and its use to assess global and regional reference crop evaporation over land during the twentieth century. *J Hydrometeorol* 12(5):823–848.
57. Hagemann S, et al. (2011) Impact of a statistical bias correction on the projected hydrological changes obtained from three GCMs and two hydrology models. *J Hydrometeorol* 12(4):556–578.
58. Kaye NR, Hartley A, Hemming D (2012) Mapping the climate: Guidance on appropriate techniques to map climate variables and their uncertainty. *Geoscientific Model Development* 5(1):245–256.

Multi-model assessment of water scarcity under climate change

Jacob Schewe ^{*}, Jens Heinke ^{* a}, Dieter Gerten ^{*}, Ingjerd Haddeland [†], Nigel W. Arnell [‡], Douglas B. Clark [§], Rutger Dankers [¶], Stephanie Eisner ^{||}, Balázs Fekete ^{**}, Felipe J. Colón-González ^b, Simon N. Gosling ^{††}, Hyungjun Kim ^{‡‡}, Xingcai Liu ^{§§}, Yoshimitsu Masaki ^{¶¶}, Felix T. Portmann ^{***}, Yusuke Satoh ^{†††}, Tobias Stacke ^{†††}, QiuHong Tang ^{§§}, Yoshihide Wada ^{§§§}, Dominik Wisser ^c, Torsten Albrecht ^{*}, Katja Frieler ^{*}, Franziska Piontek ^{*}, Lila Warszawski ^{*}, and Pavel Kabat ^{¶¶¶}

^{*}Potsdam Institute for Climate Impact Research, Potsdam, Germany, ^aInternational Livestock Research Institute, Nairobi, Kenya, [†]Norwegian Water Resources and Energy Directorate, Oslo, Norway, [‡]Walker Institute for Climate System Research, University of Reading, Reading, UK, [§]Centre for Ecology & Hydrology, Wallingford, UK, [¶]Met Office Hadley Centre, Exeter, UK, ^{||}Center for Environmental Systems Research (CESR), University of Kassel, Kassel, Germany, ^{**}Civil Engineering Department, The City College of New York, New York, USA, ^bAbdus Salam International Centre for Theoretical Physics, Trieste, Italy, ^{††}School of Geography, University of Nottingham, Nottingham, UK, ^{‡‡}Institute of Industrial Science, The University of Tokyo, Tokyo, Japan, ^{§§}Institute of Geographic Sciences and Natural Resources Research, Chinese Academy of Sciences, Beijing, China, ^{¶¶}Center for Global Environmental Research, National Institute for Environmental Studies, Tsukuba, Japan, ^{***}Biodiversity and Climate Research Centre (LOEWE BiK-F) & Senckenberg Research Institute and Natural History Museum, Frankfurt am Main, Germany; and Institute of Physical Geography, Goethe University Frankfurt, Frankfurt am Main, Germany, ^{†††}Department of Civil Engineering, The University of Tokyo, Tokyo, Japan, ^{†††}Max Planck Institute for Meteorology, Hamburg, Germany, ^{§§§}Department of Physical Geography, Utrecht University, Utrecht, Netherlands, ^cCenter for Development Research, University of Bonn, Bonn, Germany, and ^{¶¶¶}International Institute for Applied Systems Analysis, Laxenburg, Austria & Wageningen University and Research Centre, Wageningen, Netherlands

Supporting Information

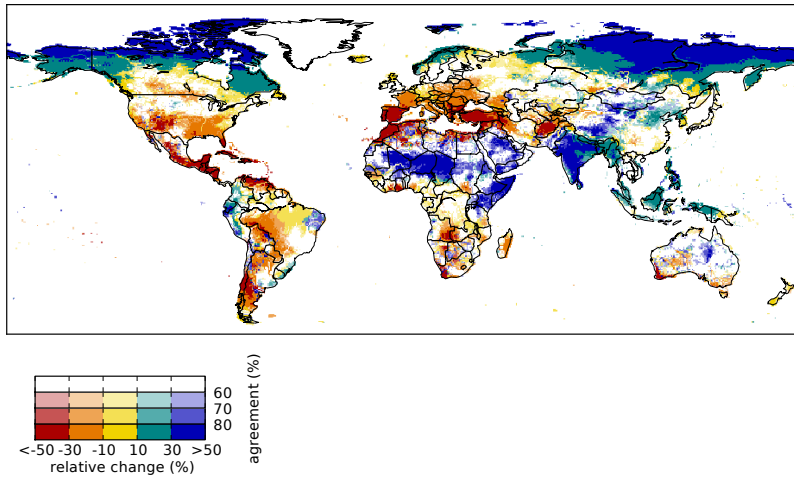


Fig. S1. As Fig. 1 (upper panel) in the main text, but for a warming of 3°C.

Table S1. Middle years of 31-year periods corresponding to the different levels of global warming (compared to present-day, i.e. the 1980–2010 average) in the individual GCMs under RCP8.5. Population projections for these same years were used, except at the 0°C level which was assumed to correspond to year-2000 population

warming level	HadGEM2-ES	IPSL-CM5A-LR	MIROC-ESM-CHEM	GFDL-ESM2M	NorESM1-M
0°C	1995	1995	1995	1995	1995
1°C	2021	2027	2023	2040	2035
2°C	2044	2047	2043	2071	2062
3°C	2062	2065	2061	-	2086*

*A 27-year period from 2073–2099 was used.

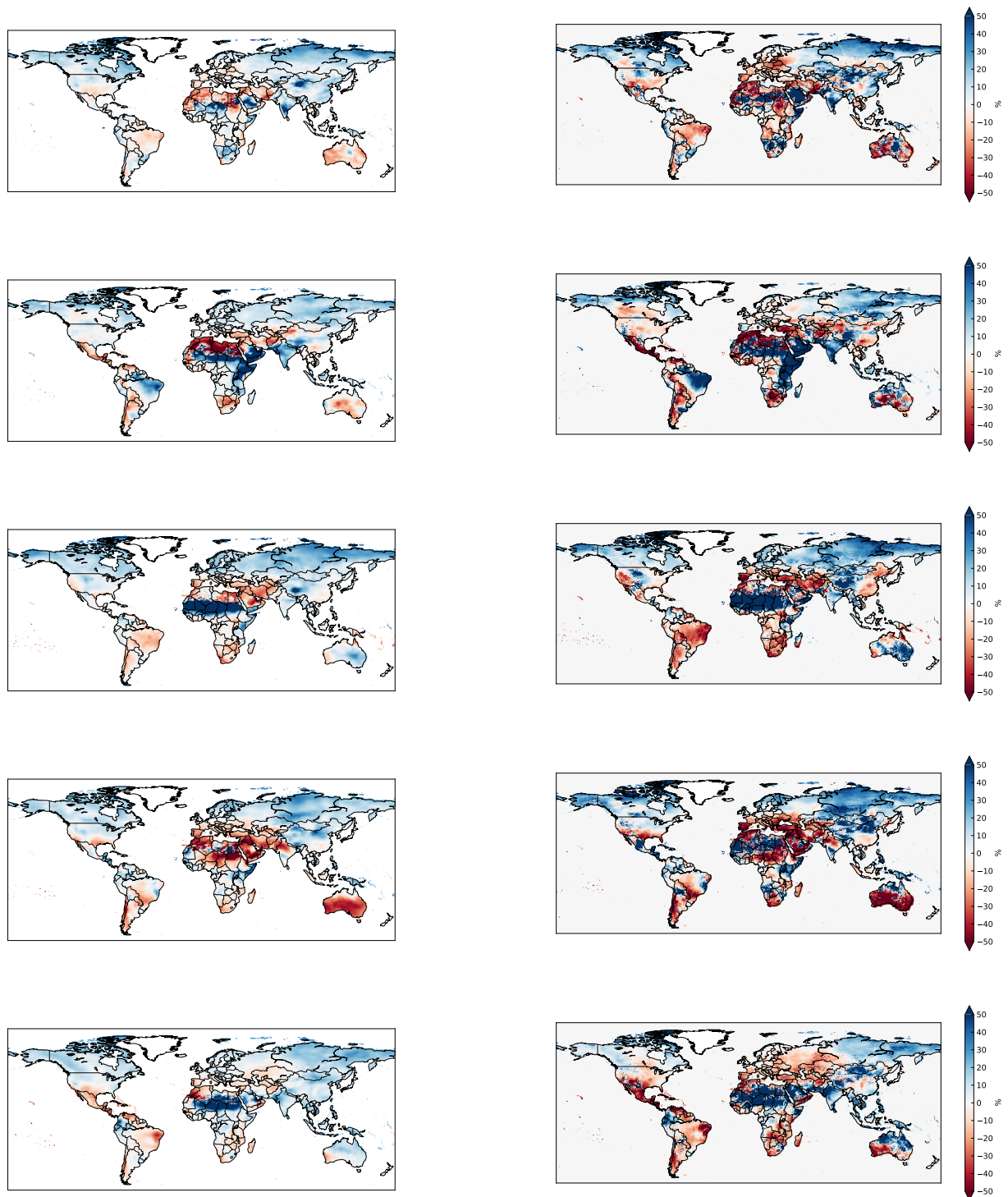


Fig. S2. Relative change in precipitation (left) and discharge (right; average over all GHMs) at 2°C compared to present-day, under RCP8.5, for (top to bottom) HadGEM2-ES, IPSL-CM5A-LR, MIROC-ESM-CHEM, GFDL-ESM2M, and NorESM1-M.

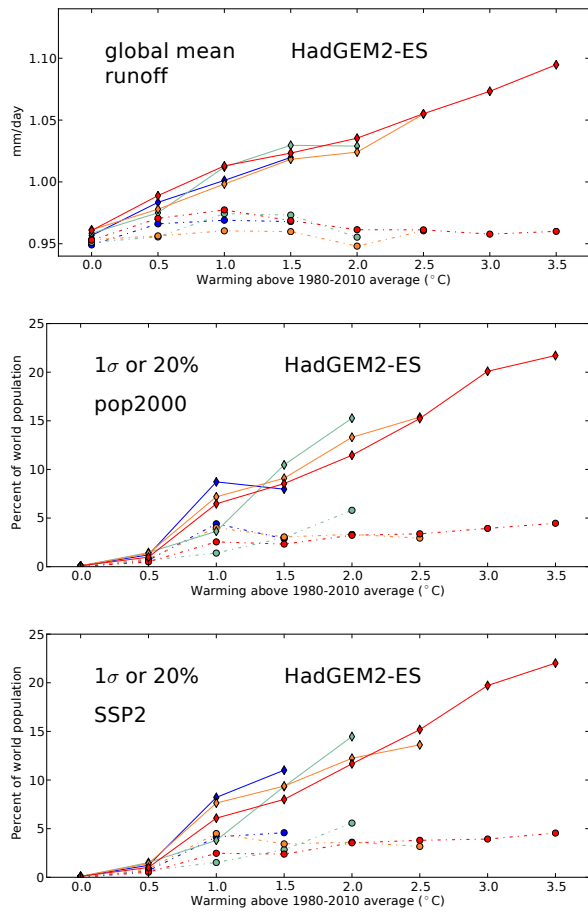


Fig. S3. Effect of different rates of global warming on global impact metrics. Shown are results for one GCM (HadGEM2-ES), two GHMs (solid and dotted lines) and all four RCPs (RCP2.6, dark blue; RCP4.5, turquoise; RCP6.0, orange; RCP8.5, red) at different levels of global warming. Upper panel: Globally averaged runoff. Middle and lower panel: Same metric as shown in Fig. 2 (upper panel) in the main paper. Middle panel: Assuming constant present-day (2010) population. Lower panel: Assuming population change according to SSP2.

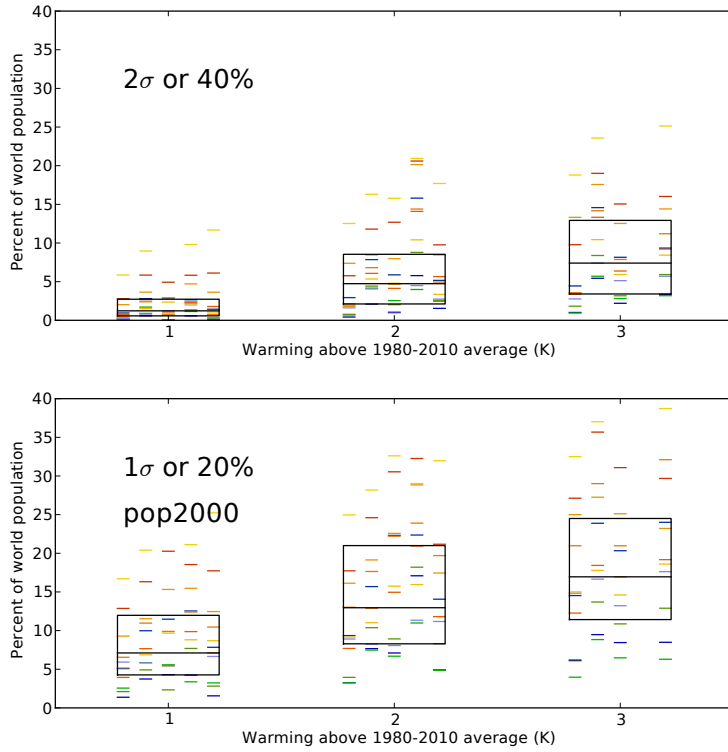


Fig. S4. As upper panel of Fig. 2 in the main paper, but (upper panel) for a reduction by more than 2σ or by more than 40%; and (lower panel) assuming constant year-2000 population.

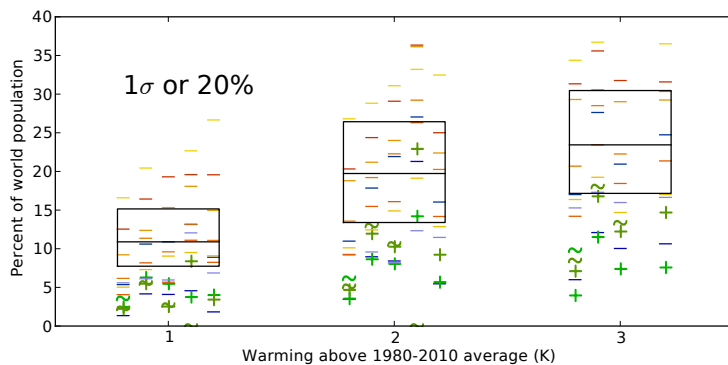


Fig. S5. As upper panel of Fig. 2 in the main paper, but with the quartiles and median (shown by the black boxes) computed without the models that include vegetation dynamics (JULES and LPJmL). The individual results of those models are highlighted in green colors, where + denotes runs with varying atmospheric CO₂ concentration, and ~ denotes runs where CO₂ concentration has been varied according to historical values up until the year 2000, and held constant at the year-2000 level thereafter.

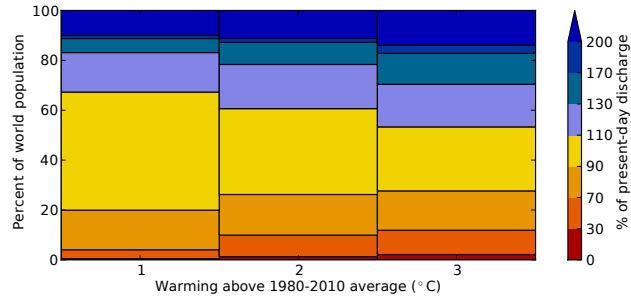


Fig. S6. Population affected by different levels of discharge increase or decrease. Shown is the multi-model mean of the percentage of the world population living in grid cells where 31-year average discharge is a certain percentage of present-day (1980–2010) discharge, at 1°C, 2°C, and 3°C of global warming, under RCP8.5 and SSP2.

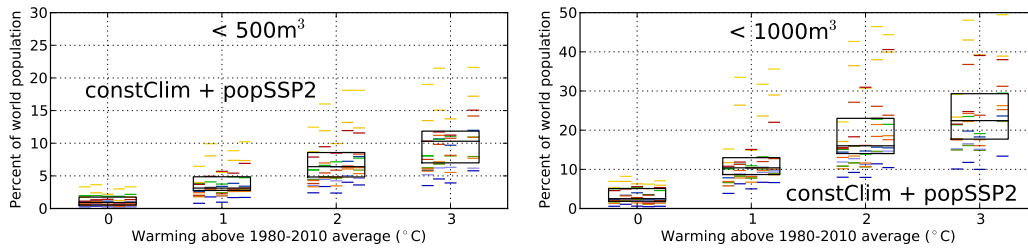


Fig. S7. As Fig. 3a and b in the main paper, but using a “Constant climate” scenario (1980–2010 average discharge). SSP2 population data from the same years as in Fig. 3a and b are used, relating the population time series to the temperature axis via the RCP8.5.

Table S2: Main characteristics of the GHMs as used in this study, based on (1).

Model name	Time step length	Meteorological forcing ^a	Energy balance	Evaporation scheme ^b	Runoff scheme ^c	Snow scheme	Vegetation dynamics	CO ₂ effect ^d	References
DBH	1h	P, T, W, Q, LW, SW, SP	Yes	Energy balance	Infiltration excess	Energy balance	No	Constant	(2, 3)
H08	Daily	R, S, T, W, Q, LW, SW, SP	Yes	Bulk formula	Saturation excess, non-linear	Energy balance	No	No	(4, 5)
JULES	30 mins	R, S, T, W, Q, LW, SW, SP	Yes	Penman-Monteith	Infiltration excess, saturation excess, groundwater.	Energy balance	Yes	Varying	(6, 7)
LPJmL	Daily	P, T, LW _n , SW	No	Priestley-Taylor	Saturation excess	Degree-day	Yes	Varying	(8, 9)
Mac-PDM.09	Daily	P, T, W, Q, LW _n , SW	No	Penman-Monteith	Saturation excess, non-linear	Degree-day	No	No	(10, 11)
MATSIRO	1 hr	R, S, T, W, Q, LW, SW, SP	Yes	Bulk formula	Infiltration excess, saturation excess, groundwater.	Energy balance	No	Constant	(12, 13)
MPI-HM	Daily	P, T, W, Q, LW _n , SW, SP	No	Penman-Monteith	Saturation excess, non-linear	Degree-day	No	No	(14, 15)
PCR-GLOBWB	Daily	P, T	No	Hamon	Saturation Excess Beta Function	Degree Day	No	No	(16–18)
VIC	Daily, 3hr snow	P, T, W, Q, LW, SW, SP.	Only for snow.	Penman-Monteith	Saturation excess, non-linear	Energy balance.	No	No	(19, 20)
WaterGAP	Daily	P, T, LW _n , SW	No	Priestley-Taylor	Beta function	Degree day	No	No	(21–23)
WBM	Daily	P, T	No	Hamon	Saturation Excess	Empirical temp and precip based formula	No	No	(24, 25)

^a R: rainfall rate, S: snowfall rate, P: precipitation rate (rain and snow calculated in the model), T: air temperature, W: wind speed, Q: air specific humidity, LW: downwelling longwave radiation; LW_n: net longwave radiation; SW: downwelling shortwave radiation, SP: surface pressure.

^b Bulk formula: Bulk transfer coefficients are used when calculating turbulent heat fluxes.

^c Non-linear: Subsurface runoff is a non-linear function of soil moisture.

^d CO₂ concentration in calculation of stomatal conductance.

Supplementary References

1. Haddeland I et al. (2011) Multimodel Estimate of the Global Terrestrial Water Balance: Setup and First Results. *Journal of Hydrometeorology* 12:869–884.
2. Tang Q, Oki T, Kanae S, Hu H (2007) The Influence of Precipitation Variability and Partial Irrigation within Grid Cells on a Hydrological Simulation. *Journal of Hydrometeorology* 8:499–512.
3. Tang Q, Oki T, Kanae S, Hu H (2008) Hydrological Cycles Change in the Yellow River Basin during the Last Half of the Twentieth Century. *Journal of Climate* 21:1790–1806.
4. Hanasaki N et al. (2008) An integrated model for the assessment of global water resources – Part 1: Model description and input meteorological forcing. *Hydrology and Earth System Sciences* 12:1007–1025.
5. Hanasaki N et al. (2008) An integrated model for the assessment of global water resources – Part 2: Applications and assessments. *Hydrology and Earth System Sciences* 12:1027–1037.
6. Best MJ et al. (2011) The Joint UK Land Environment Simulator (JULES), model description – Part 1: Energy and water fluxes. *Geoscientific Model Development* 4:677–699.
7. Clark DB et al. (2011) The Joint UK Land Environment Simulator (JULES), Model description – Part 2: Carbon fluxes and vegetation. *Geoscientific Model Development Discussions*.
8. Bondeau A et al. (2007) Modelling the role of agriculture for the 20th century global terrestrial carbon balance. *Global Change Biology* 13:679–706.
9. Rost S et al. (2008) Agricultural green and blue water consumption and its influence on the global water system. *Water Resources Research* 44:1–17.
10. Arnell N. (1999) A simple water balance model for the simulation of streamflow over a large geographic domain. *Journal of Hydrology* 217:314–335.
11. Gosling SN, Arnell NW (2011) Simulating current global river runoff with a global hydrological model: model revisions, validation, and sensitivity analysis. *Hydrological Processes* 25:1129–1145.
12. Takata K, Emori S, Watanabe T (2003) Development of the minimal advanced treatments of surface interaction and runoff. *Global and Planetary Change* 38:209–222.
13. Pokhrel Y et al. (2012) Incorporating Anthropogenic Water Regulation Modules into a Land Surface Model. *Journal of Hydrometeorology* 13:255–269.
14. Hagemann S, Dümenil Gates L (2003) Improving a subgrid runoff parameterization scheme for climate models by the use of high resolution data derived from satellite observations. *Climate Dynamics* 21:349–359.
15. Stacke T, Hagemann S (2012) Development and validation of a global dynamical wetlands extent scheme. *Hydrology and Earth System Sciences Discussions* 9:405–440.

16. Wada Y et al. (2010) Global depletion of groundwater resources. *Geophysical Research Letters* 37:L20402.
17. Van Beek LPH, Wada Y, Bierkens MFP (2011) Global monthly water stress: 1. Water balance and water availability. *Water Resources Research* 47:W07517.
18. Wada Y et al. (2011) Global monthly water stress: 2. Water demand and severity of water stress. *Water Resources Research* 47:W07518.
19. Liang X, Lettenmaier DP, Wood EF, Burges SJ (1994) A simple hydrologically based model of land surface water and energy fluxes for general circulation models. *Journal of Geophysical Research* 99:14415.
20. Lohmann D, Raschke E (1998) Regional scale hydrology: I. Formulation of the VIC-2L model coupled to a routing model. *Hydrological Sciences Journal* 43:131–141.
21. Döll P et al. (2012) Impact of water withdrawals from groundwater and surface water on continental water storage variations. *Journal of Geodynamics* 59–60:143–156.
22. Döll P, Kaspar F, Lehner B (2003) A global hydrological model for deriving water availability indicators: model tuning and validation. *Journal of Hydrology* 270:105–134.
23. Flörke M et al. (2013) Domestic and industrial water uses of the past 60 years as a mirror of socio-economic development: A global simulation study. *Global Environmental Change* 23:144–156.
24. Vörösmarty CJ, Federer CA, Schloss AL (1998) Potential evaporation functions compared on US watersheds: Possible implications for global-scale water balance and terrestrial ecosystem modeling. *Journal of Hydrology* 207:147–169.
25. Wisser D, Fekete BM, Vörösmarty CJ, Schumann AH (2010) Reconstructing 20th century global hydrography: a contribution to the Global Terrestrial Network- Hydrology (GTN-H). *Hydrology and Earth System Sciences* 14:1–24.